ACS APPLIED MATERIALS & INTERFACES

Research Article

www.acsami.org

A Ligation Dnazyme-Induced Magnetic Nanoparticles Assembly for Ultrasensitive Detection of Copper Ions

Honghong Yin,[†] Hua Kuang,*[,†] Liqiang Liu, Liguang Xu, Wei Ma, Libing Wang, and Chuanlai Xu

State Key Lab of Food Science and Technology, School of Food Science and Technology, Jiangnan University, Wuxi, Jiangsu 214122, China

ABSTRACT: A novel biosensor for ultrasensitive detection of copper (Cu^{2+}) was established based on the assembly of magnetic nanoparticles induced by the Cu^{2+}-dependent ligation DNAzyme. With a low limit of detection of 2.8 nM and high specificity, this method has the potential to serve as a general platform for the detection of heavy metal ions.

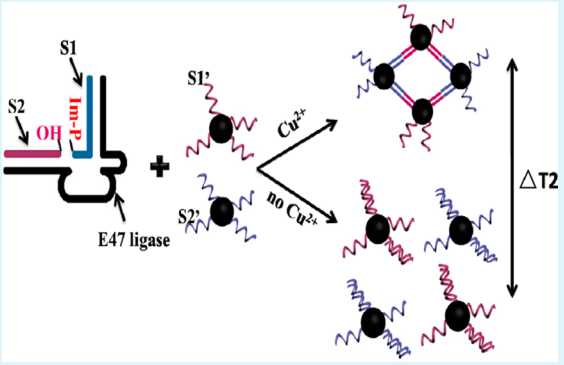

KEYWORDS: *MRI sensor, ligation DNAzyme, copper ions*

1. INTRODUCTION

Copper is the third most essential transition metal for human health after zinc and iron and acts as a cofactor or structural component of certain proteins producing numerous enzymes critical for life.[1] Copper is also a micronutrient required for multiple functions including bone formation, cellular respiration, and connective tissue development.[2] However, elevated concentrations of Cu^{2+} may lead to adverse effects in organisms, resulting in gastrointestinal distress, liver or kidney damage, and serious neurodegenerative diseases, such as Menkes disease, Wilson disease, and Alzheimer's disease.[3−6] Therefore, it is of considerable significance to establish highly sensitive and effective methods to monitor the Cu^{2+} level in water.

The safety limit of Cu^{2+} in drinking water set by the U.S. Environmental Protection Agency (EPA) is 1.3 ppm (20 mM).[7] Various technologies have been developed for the detection of Cu^{2+}. The standard procedures for Cu^{2+} detection are instrument-based analytical methods, such as inductively coupled plasma (ICP) and graphite furnace atomic absorption spectroscopy.[8,9] However, high equipment costs and specialized personnel are required, resulting in the restriction of their application during routine detection. The electrochemical and optical methods were also used for Cu^{2+} detection, but a higher sensitivity still needed to be improved.[10−12] With the advent of new detection methods, fluorescence sensors and colorimetric sensors based on fluorescence probes, organic dyes, or nanomaterials as new approaches have attracted more attention.[13−19] Chen et al. reported a colorimetric method for the detection of trace copper ions based on the catalytic leaching of silver-coated gold nanoparticles, and the limit of detection (LOD) reached a low level of 1 nM.[20] However, the color was easily influenced by the reaction system, resulting in the appearance of false-positive results. In addition, DNAzyme-based detection strategies have been used for Cu^{2+} recognition and signal generation, which has led to new detection methods in research tests. Cleavage-based DNAzyme has been used most frequently.[21−23] Lu et al. first used a ligation DNAzyme-based method for colorimetric Cu^{2+} detection, with sensitivity at the micromolar level. This ligation DNAzyme had many advantages over cleavage-based DNAzyme, as it was less susceptible to nonspecific samples and showed zero background detection.[24,25]

With the development of nanomaterials,[26−30] magnetic nanoparticles (MNPs)-based magnetic resonance imaging (MRI) for the detection of harmful substances has attracted considerable interest. The MRI technology has many advantages over other systems. First, a significant improvement of the sensitivity can be obtained by this method. Second, different samples can be detected on the nuclear resonance instrument simultaneously, which can realize high throughput analysis. In addition, the obtained MRI images can easily assess the detection result by naked eyes.[31−35] MNPs are important nanomaterials with multiple fundamental properties, including superparamagnetism, high magnetization, high coercivity, and a macroscopic quantum tunneling effect and can be easily modified by other molecules due to the functionalized groups on their surface.[36,37] They are mainly used in bioseparation, enrichment, drug delivery, diagnosis and treatment of diseases, and MRI.[38−41] MRI is a powerful technique and is widely used

Received: December 1, 2013
Accepted: March 10, 2014
Published: March 10, 2014

in clinical diagnosis and biodetection and can accurately locate the absence of molecules in some tissues, and the results are reflected in the MRI images. MNPs as contrast agents have fabricated numerous MRI sensors for the detection of harmful elements, and the application of MNPs has been extended to food safety, environmental protection, and many other fields.

In the present study, we established a novel method for the ultrasensitive detection of Cu^{2+} based on the aggregation of MNPs induced by the Cu^{2+}-dependent DNA ligation DNAzyme. The structure of the DNAzyme is shown in Scheme 1 and consisted of three nucleotide sequences, namely

Scheme 1. Scheme of the Ligation DNAzyme-based MRI Sensor for Cu^{2+} Detection

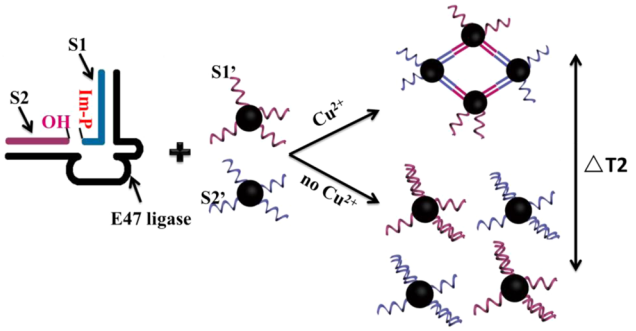

the enzyme strand E47, substrate S1, and substrate S2. Under optimized conditions, a low LOD of 2.8 nM was obtained, which was much lower than the detection level reported by Lu.[21] To the best of our knowledge, this is the first report on the development of an MRI sensor for Cu^{2+} detection based on ligation DNAzyme.

2. EXPERIMENTAL SECTION

2.1. Materials and Reagents. The Fe_3O_4 magnetic nanoparticles were purchased from Beijing Oneder Hightech Co., Ltd. Imidazole, 1-ethyl-3-(3-dimethyl aminopropyl) carbodiimide hydrochloride (EDC), and *N*-hydroxy succinimide (NHS) were obtained from Sigma-Aldrich. Tris-acetate buffer (pH 8.2) was from Shengon Biotechnology Co., Ltd. (Shanghai, China). Other chemicals of analytical grade were purchased from J&K Scientific Ltd. (Beijing, China). Deionized water used throughout the experiment was purified to 18.2 MW (Millipore). All the DNA fragments were synthesized by Shengon Biotechnology Co., Ltd. (Shanghai, China) and purified by HPLC. Their detailed sequences are as follows:

S1: 5′-AAGCATCTCAAGC-3′
S2: 5′-GGAACACTATCCG-3′
S1′: 5′-GCTTGAGATGCTTAAAAAAAAAA-NH_2-3′
S2′: 5′-NH_2-AAAAAAAAAACGGATAGTGTTCC-3′
E47: 5′-CGGATAGTGTTCTTTCGCTAGACCATGTGA-CGCATGGTGAGATGCTT-3′
AntiE47: 5′-ACCATGCGTCACATGGTCTAGCGAAAGAA-3′

2.2. Preparation of DNA-modified MNPs. The Fe_3O_4 magnetic nanoparticles with a diameter of 10.3 ± 1.6 nm were functionalized with carboxyl groups on the surface and showed excellent dispersibility (Figure 3a). The carboxyl group functionalized MNPs are possessed of negative charge; the electrostatic repulsion between MNPs would not lead to charge accumulation. Therefore, for a short time, the MNPs would not aggregate with time and temperature. The MNPs and DNA were connected by EDC and NHS. Typically, 0.15 mg of Fe_3O_4 nanoparticles (about 10 nM) was dissolved in 100 μL of PBS (containing 0.01 M sodium phosphate and 50 mM NaCl), followed by the addition of 0.0746 mg of EDC and 0.12 mg of NHS. Half an hour later, the complementary sequences of S1 and S2 (S1′ and S2′) were respectively added to the MNPs at a final concentration of 2 μM. After gentle shaking for 4 h at room temperature, the excess DNA was removed by ultrafiltration using a 3000 MW cutoff membrane. To ensure the DNA was completely removed, this procedure was performed three times at 10 000 r/min for 5 min each time. The MNPs were then resuspended in Tris-acetate buffer (25 mM, pH 7.2).

2.3. Construction and NMR Measurement of the DNAzyme-based MRI Sensor. To help in combining the S1 and S2, the S1 was first activated by imidazole. A 20 μL volume of 100 μM S1 was reacted with 2.5 μL of 1 μM imidazole (pH 6.0) and 2.5 μL of 1.5 M EDC·HCl at room temperature for 1 h, resulting in the attachment of an imidazole group to the 3-phosphate group of S1. The solution was then purified by ultrafiltration, and the concentration was measured by monitoring the absorbance at 260 nm.

To establish the DNAzyme-based MRI sensor, imidazole-activated S1, S2, and E47 (1 μM of each) were dissolved in 30 mM HEPES buffer (containing 30 mM KCl and 20 mM $MgCl_2$, pH 7.0). Then, 1 μL of different concentrations of Cu^{2+} (5, 20, 50, 100, 200, 500, and 1000 nM) was added to 100 μL of the above mixture to induce the ligation reaction between S1 and S2. After 30 min, the S1 and S2 became one complete DNA sequence (S1−S2), and the terminal bases of E47 were hybridized to S1−S2. Then, 50 μL of the above solution was mixed with 50 μL of DNA-modified MNPs (25 μL MNPs-S1′, 25 μL MNPs-S2′) and 2 μM of AntiE47 DNA and placed in boiling water and allowed to cool to room temperature in 30 min. After the reaction, the AntiE47 DNA hybridized with the middle single strand of E47, resulting in the dissociation of S1−S2 from E47. The MNPs would be assembled through the hybridization of DNA on the surface of MNPs and the single S1−S2. In the end, the T2 relaxation time of MNP assembly was measured with a NMI20-analyst (Niumag Corp., Shanghai, China) at room temperature.

2.4. Specificity Tests. The specificity and selectively of this method for other metal ions, including Mn^{2+}, Zn^{2+}, Mg^{2+}, Fe^{2+}, Ca^{2+}, Hg^{2+}, and Pb^{2+}, was performed at a concentration of 10 nM. Using the same detection procedure, the T2 relaxation time was determined for each metal ion and compared with that for Cu^{2+}.

2.5. Recovery in Drinking Water Samples. To evaluate the feasibility of the sensor in practical sample detection, a recovery test was performed in drinking water. Using 5, 10, 20, 50, 100, and 200 nM standard samples, the T2 values were measured, and the recovery was calculated.

3. RESULTS AND DISCUSSION

The sensing principle for the detection of Cu^{2+} is illustrated in Scheme 1. First, the S1 is activated with imidazole, and then the S1 and S2 are hybridized to the 5′ and 3′ region of E47, respectively. In the presence of Cu^{2+}, the phosphorus center of S1 and the hydroxyl group of S2 undergo nucleophilic attack by the catalyst of E47, and the imidazole group is left due to the formation of the phosphodiester bond. The DNA sequence of AntiE47 is complementary with 29 bases on E47, which contribute to dissociation of the ligated substrate from E47. The complete ligated substrate is further hybridized with S1′ and S2′, which were then coupled to MNPs, resulting in the aggregation of MNPs. In the absence of Cu^{2+}, no aggregation occurred due to the unconnected substrate strand. The role of MNPs in this work acts as contrast agent. Under different aggregations of MNPs, the magnetic relaxation properties of surrounding water protons of MNPs were different, resulting in the variation of spin−spin relaxation time (T2) with different MNP assembly mediated by Cu^{2+}. Therefore, the T2 relaxation time was used as the detection signal to quantify the content of targets.

To ensure the successful combination of MNPs and DNA fragments, dynamic light scattering (DLS) was used to measure the size difference between the naked Fe_3O_4 particles and the

assembly of MNPs and DNA. As shown in Figure 1, the hydrodynamic size of the MNPs-DNA increased compared

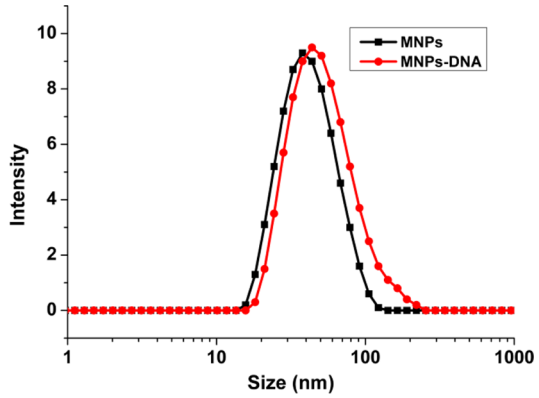

Figure 1. The size change of MNPs before and after DNA conjugation. 1, the original MNPs; 2, the MNPs modified with DNA.

with MNPs, which indicated that the carboxyl-functionalized MNPs and amino-modified DNA sequence were successfully prepared.

To obtain optimum detection results using the MRI sensor, the concentration of DNAzyme, which has a direct relationship with the aggregation level of MNPs, was optimized. At 10 nM of MNPs-DNA and 2 μM of AntiE47 DNA, the concentration of imidazole-activated S1, S2, and E47 changed from 100 nM to 2 μM. As seen in Figure 2, the T2 value almost reached a

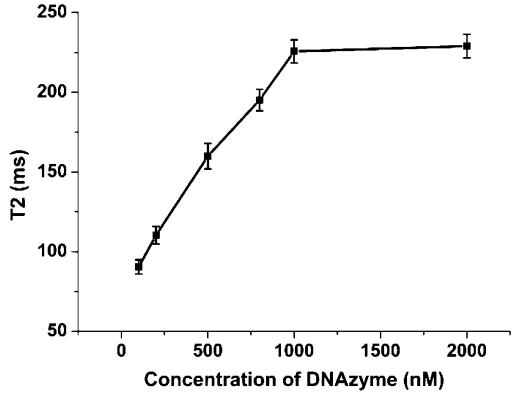

Figure 2. Effect of the concentration of DNAzyme on T2 values (100, 200, 500, 800, 1000, 2000 nM).

saturation level at a concentration of 1 μM. Therefore, 1 μM of DNAzyme (each of the three DNA strands) was enough for construction of the MRI sensor.

The typical transmission electron microscopy (TEM) images of the MNPs assembly showed the degree of aggregation of different amounts of Cu^{2+} (0, 5, 100, 500 nM). As the concentration of Cu^{2+} increased, aggregation of the monodispersed MNPs increased (Figure 3). In addition, DLS was performed to estimate the typical size distributions of the MNP aggregates. As shown in Figure 4A, the peak location of the distribution curve of particle size increased with the increasing concentration of Cu^{2+}, which represented that the size of MNPs assembly showed a growth trend with the increased Cu^{2+} concentrations ranging from 0 to 1000 nM (Figure 4B). An obvious variation was seen between low and high concentrations of Cu^{2+}. The width of the curve represents

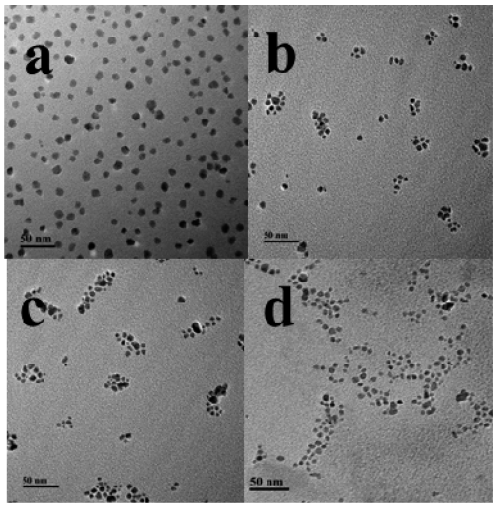

Figure 3. Typical TEM images of MNPs and MNP assembly under different concentrations of Cu^{2+}. (a) naked MNPs, (b) MNP assembly in the presence of 5 nM of Cu^{2+}, (c) MNP assembly in the presence of 100 nM of Cu^{2+}, (d) MNP assembly in the presence of 500 nM of Cu^{2+}.

the polymey disperse index (PDI) of particles, which means the monodispersity of the MNPs assembly. All the PDI of the curves were about 0.2, which means that the monodispersity of the samples was excellent and the width of the distribution curve has no relationship with the size of particles influenced by the concentrations of Cu^{2+}. Therefore, the increased size of the MNPs with increasing concentrations of Cu^{2+} could be characterized by the peak location of the curve. The TEM images and size distributions indicated the successful assembly of MNPs in the presence of Cu^{2+}.

At Cu^{2+} concentrations ranging from 1 nM to 1000 nM, the sensitivity of the method was determined using this sensor. Shown in Figure 5, the inserted image, the T2 values increased with the increase of Cu^{2+} concentration. At less than a 5 nM Cu^{2+} concentration, the T2 values were lower and the variation was not obvious. In the range of 5 nM to 1000 nM, the MR images shown in Figure 6A claimed that the color became brighter with the increased aggregation of MNPs. Meanwhile, a good linear relationship of T2 values versus Cu^{2+} concentration was obtained, and an LOD of 2.8 nM was calculated from the dose−response curve with a good coefficient of 0.9908 (Figure 5).

A specificity test using other metal ions (Mn^{2+}, Zn^{2+}, Mg^{2+}, Fe^{2+}, Ca^{2+}, Hg^{2+}, Pb^{2+}) as detection substances was performed to analyze the variation in T2 values. As shown in Figure 6B, at a concentration of 10 nM, the first metal detected was Cu^{2+}, which showed a brighter color than other samples. Taking Pb^{2+} as an example, the T2 values with about 10 ms showed no obvious variation under the concentrations of 5 nM to 1000 nM in Figure 5, so as the other metal ions. All the above results demonstrated that the other metal ions did not influence the Cu^{2+}-dependent DNAzyme, and the MNPs assembly was not formed. Therefore, this method had excellent specificity for the detection of target Cu^{2+}.

A recovery test was performed in drinking water to evaluate the feasibility and reproducibility of the sensor. Different concentrations of Cu^{2+} (5, 10, 20, 50, 100, 200 nM) were added to the detection system. As shown in Table 1, satisfactory recovery in the range of 89.9 to 96.3% was obtained and

dx.doi.org/10.1021/am405482a | ACS Appl. Mater. Interfaces 2014, 6, 4752−4757

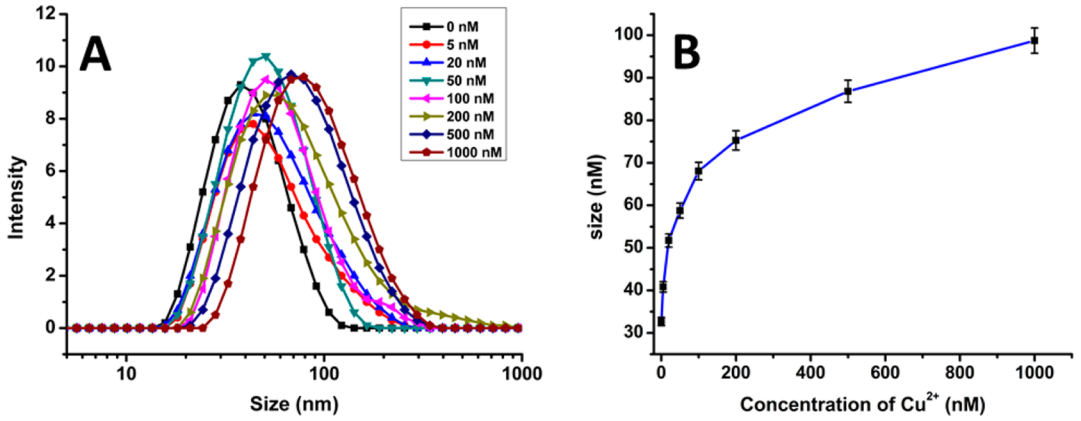

Figure 4. (A) Typical hydrodynamic size distributions of the MNP assembly under different concentrations of Cu^{2+} in the range of 0 to 1000 nM. (B) The growth trend of the MNP assembly size under the concentrations of Cu^{2+} ranging from 0 to 1000 nM.

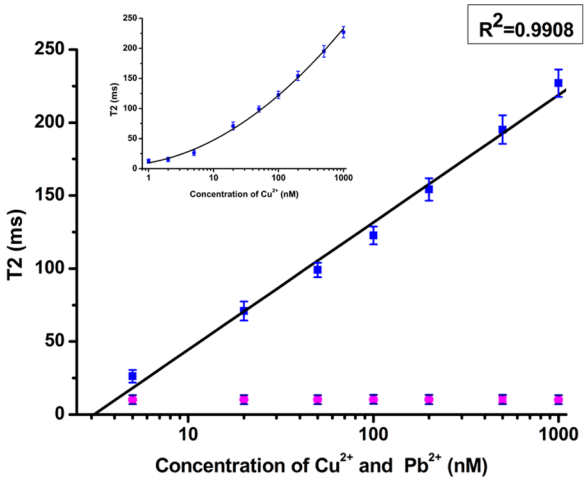

Figure 5. The standard curve for the detection of Cu^{2+} in the range of 5 to 1000 nM. A dose−response plot for the detection of Cu^{2+} at concentrations of 1 to 1000 nM (the inserted image). A scatterplot of Pb^{2+} detection under concentrations of 5 to 1000 nM.

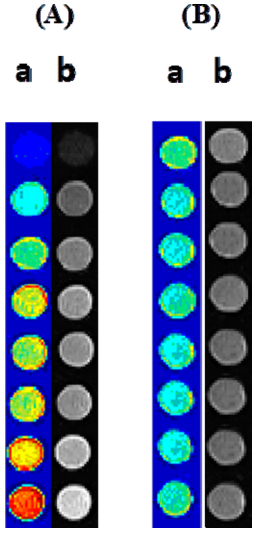

Figure 6. The T2 values images (a) and MR images (b) of the detection. (A) The detection of Cu^{2+}: from top to bottom, the concentrations of Cu^{2+} were 5, 20, 50, 100, 200, 500, and 1000 nM. (B) The specificity test: from top to bottom, Cu^{2+}, Mn^{2+}, Zn^{2+}, Mg^{2+}, Fe^{2+}, Ca^{2+}, Hg^{2+}, Pb^{2+}, ;the concentration of the reference ions were all 10 nM.

confirmed that this sensor is a powerful tool for the detection of Cu^{2+} in real samples.

4. CONCLUSIONS

In conclusion, a novel method for the highly sensitive detection of Cu^{2+} was established based on the aggregation of MNPs induced by the Cu^{2+}-dependent DNA ligation DNAzyme. Cu^{2+} played a significant role in ligation of the substrate strand, which resulted in the formation of the MNPs assembly. Compared with the work by Lu, the detection signals were different between the two approaches, Lu used extinction spectra, and we used the NMR signal. The NMR signal was much more sensitive than extinction spectra. Under the same aggregation level, the NMR signal showed an obvious change compared with the extinction spectra. Even at lower concentrations of targets, the NMR signal still had distinct signal variation, while the extinction spectra signal may keep the same level. Therefore, the sensitivity in our work presented substantial increase. In the quantitative analysis of Cu^{2+}, a low LOD of 2.8 nM was obtained in the range of 5 to 1000 nM, which is below the safety limit set by the U.S. EPA. In addition, excellent selectivity was confirmed by the detection of other metal ions, and satisfactory recovery in real samples was obtained, which proved that this sensor has great potential in the detection of metal ions.

Table 1. Determination of Cu^{2+} in Drinking Water

spiked concentration (nM)	detected concentration recovery (%)	mean[a] ± SD[b] (nM)
200	182.657 ± 18.49	91.3
100	92.88 ± 9.462	92.9
50	44.952 ± 3.580	89.9
20	18.346 ± 1.563	91.7
10	9.627 ± 0. 68	96.3
5	4.965 ± 0.29	93

[a]The mean of three experiments. [b]SD = standard deviation.

AUTHOR INFORMATION

Corresponding Author

*E-mail: kuangh@jiangnan.edu.cn.

Author Contributions

†These authors contributed to this paper equally.

Notes

The authors declare no competing financial interest.

■ ACKNOWLEDGMENTS

This work is financially supported by the Key Programs from MOST (2012AA06A303, 2012BAD29B04).

■ REFERENCES

(1) Wu, S. P.; Huang, R. Y.; Du, K. J. Colorimetric Sensing of Cu (II) by 2-methyl-3-[(pyridin-2-ylmethyl)-amino]-1, 4-naphthoquinone: Cu (II) Induced Deprotonation of NH Responsible for Color Changes. *Dalton Trans.* **2009**, *24*, 4735−4740.

(2) Viguier, R. F.; Hulme, A. N. A Sensitized Europium Complex Generated by Micromolar Concentrations of Copper (I): toward the detection of copper (I) in biology. *J. Am. Chem. Soc.* **2006**, *128*, 11370−11371.

(3) Barnham, K. J.; Masters, C. L.; Bush, A. I. Neurodegenerative Diseases and Oxidative Stress. *Nat. Rev. Drug Discovery* **2004**, *3*, 205−214.

(4) Domaille, D. W.; Que, E. L.; Chang, C. J. Synthetic Fluorescent Sensors for Studying the Cell Biology of Metals. *Nat. Chem. Biol.* **2008**, *4*, 168−175.

(5) Kim, Y. R.; Kim, H. J.; Kim, J. S.; Kim, H. Rhodamine-Based "Turn-On" Fluorescent Chemodosimeter for Cu (II) on Ultrathin Platinum Films as Molecular Switches. *Adv. Mater.* **2008**, *20*, 4428−4432.

(6) Qu, W.; Liu, Y.; Liu, D.; Wang, Z.; Jiang, X. Copper-Mediated Amplification Allows Readout of Immunoassays by the Naked Eye. *Angew. Chem., Int. Ed.* **2011**, *123*, 3504−3507.

(7) Rózga, M.; Kłoniecki, M.; Dadlez, M.; Bal, W. A Direct Determination of the Dissociation Constant for the Cu (II) Complex of Amyloid β 1−40 Peptide. *Chem. Res. Toxicol.* **2009**, *23*, 336−340.

(8) Freedman, Y. E.; Ronen, D.; Long, G. L. Determination of Cu and Cd Content of Groundwater Colloids by Solid Sampling Graphite Furnace Atomic Absorption Spectrometry. *Environ. Sci. Technol.* **1996**, *30*, 2270−2277.

(9) Zhu, Y.; Itoh, A.; Umemura, T.; Haraguchi, H.; Inagaki, K.; Chiba, K. Determination of REEs in Natural Water by ICP-MS with the aid of an Automatic Column Changing System. *J. Anal. Atom. Spectrom.* **2010**, *25*, 1253−1258.

(10) Lin, M.; Cho, M.; Choe, W.-S.; Son, Y.; Lee, Y. Electrochemical Detection of Copper Ion using a Modified Copolythiophene Electrode. *Electrochim. Acta* **2009a**, *54*, 7012−7017.

(11) Lin, M.; Cho, M.; Choe, W.; Lee, Y. Electrochemical Analysis of Copper Ion Using a Gly−Gly−His Tripeptide Modified Poly (3-thiopheneacetic acid) Biosensor. *Biosens. Bioelectron.* **2009b**, *25*, 28−33.

(12) Oehme, I.; Wolfbeis, O. S. Optical Sensors for Determination of Heavy Metal Ions. *Microchim. Acta* **1997**, *126*, 177−192.

(13) Chen, W.; Tu, X.; Guo, X. Fluorescent Gold Nanoparticles-based Fluorescence Sensor for Cu^{2+} Ions. *Chem. Commun.* **2009**, *13*, 1736−1738.

(14) He, X.; Liu, H.; Li, Y.; Wang, S.; Wang, N.; Xiao, J.; Xu, X.; Zhu, D. Gold Nanoparticle-Based Fluorometric and Colorimetric Sensing of Copper (II) Ions. *Adv. Mater.* **2005**, *17*, 2811−2815.

(15) Lin, W.; Long, L.; Chen, B.; Tan, W.; Gao, W. Fluorescence Turn-on Detection of Cu^{2+} in water Samples and Living Cells based on the Unprecedented Copper-mediated Dihydrorosamine Oxidation Reaction. *Chem. Commun.* **2010**, *46*, 1311−1313.

(16) Ma, Y. R.; Niu, H. Y.; Cai, Y. Q. Rapid and Sensitive Detection of Microcystin by Immunosensor based on Nuclear Magnetic Resonance. *Chem. Commun.* **2011b**, *47*, 12643−12645.

(17) Wang, H.; Wang, Y.; Jin, J.; Yang, R. Gold Nanoparticle-based Colorimetric and "Turn-on" Fluorescent Probe for Mercury (II) Ions in Aqueous Solution. *Anal. Chem.* **2008**, *80*, 9021−9028.

(18) Yin, B. C.; Ye, B. C.; Tan, W.; Wang, H.; Xie, C. C. An Allosteric Dual-DNAzyme Unimolecular Probe for Colorimetric Detection of Copper (II). *J. Am. Chem. Soc.* **2009**, *131*, 14624−14625.

(19) Zhou, Y.; Wang, S.; Zhang, K.; Jiang, X. Visual Detection of Copper (II) by Azide-and Alkyne-Functionalized Gold Nanoparticles Using Click Chemistry. *Angew. Chem., Int. Ed.* **2008**, *120*, 7564−7566.

(20) Lou, T.; Chen, L.; Chen, Z.; Wang, Y.; Chen, L.; Li, J. Colorimetric Detection of Trace Copper Ions based on Catalytic Leaching of Silver-coated Gold Nanoparticles. *ACS Appl. Mater. Interfaces* **2011**, *3*, 4215−4220.

(21) Fang, Z.; Huang, J.; Lie, P.; Xiao, Z.; Ouyang, C.; Wu, Q.; Wu, Y.; Liu, G.; Zeng, L. Lateral Flow Nucleic Acid Biosensor for Cu^{2+} Detection in Aqueous Solution with High Sensitivity and Selectivity. *Chem. Commun.* **2010**, *46*, 9043−9045.

(22) Liu, J.; Lu, Y. A DNAzyme Catalytic Beacon Sensor for Paramagnetic Cu^{2+} Ions in Aqueous Solution with High Sensitivity and Selectivity. *J. Am. Chem. Soc.* **2007b**, *129*, 9838−9839.

(23) Xu, X.; Daniel, W. L.; Wei, W.; Mirkin, C. A. Colorimetric Cu^{2+} Detection Using DNA-Modified Gold-Nanoparticle Aggregates as Probes and Click Chemistry. *Small* **2010**, *6*, 623−626.

(24) Liu, J.; Lu, Y. Colorimetric Cu^{2+} Detection with a Ligation DNAzyme and Nanoparticles. *Chem. Commun.* **2007a**, *46*, 4872−4874.

(25) Sreedhara, A.; Li, Y.; Breaker, R. R. Ligating DNA with DNA. *J. Am. Chem. Soc.* **2004**, *126*, 3454−3460.

(26) Li, Z.; Zhu, Z.; Liu, W.; Zhou, Y.; Han, B.; Gao, Y.; Tang, Z. Reversible Plasmonic Circular Dichroism of Au Nanorod and DNA Assemblies. *J. Am. Chem. Soc.* **2012**, *134*, 3322−3325.

(27) Li, X.; Zhou, Y.; Zheng, Z.; Yue, X.; Dai, Z.; Liu, S.; Tang, Z. Glucose Biosensor based on Nanocomposite Films of CdTe Quantum Qots and Glucose Oxidase. *Langmuir* **2009**, *25*, 6580−6586.

(28) Li, Z.; Cheng, E.; Huang, W.; Zhang, T.; Yang, Z.; Liu, D.; Tang, Z. Improving the Yield of Mono-DNA-functionalized Gold Nanoparticles through Dual Steric Hindrance. *J. Am. Chem. Soc.* **2011**, *133*, 15284−15287.

(29) Liu, X.; Zhang, L.; Zeng, J.; Gao, Y.; Tang, Z. Superparamagnetic Nano-immunobeads toward Food Safety Insurance. *J. Nanopart. Res.* **2013**, *15*, 1−10.

(30) Meng, H.; Yang, Y.; Chen, Y.; Zhou, Y.; Liu, Y.; Chen, X.a.; Ma, H.; Tang, Z.; Liu, D.; Jiang, L. Photoelectric Conversion Switch based on Quantum Qots with I-motif DNA Scaffolds. *Chem. Commun.* **2009**, 2293−2295.

(31) Ma, W.; Chen, W.; Qiao, R.; Liu, C.; Yang, C.; Li, Z.; Xu, D.; Peng, C.; Jin, Z.; Xu, C. Rapid and Sensitive Detection of Microcystin by Immunosensor based on Nuclear Magnetic Resonance. *Biosens. Bioelectron.* **2009**, *25*, 240−243.

(32) Ma, W.; Hao, C.; Ma, W.; Xing, C.; Yan, W.; Kuang, H.; Wang, L.; Xu, C. Wash-free Magnetic Oligonucleotide Probes-based NMR Sensor for Detecting the Hg Ion. *Chem. Commun.* **2011a**, *47*, 12503−12505.

(33) Ma, W.; Yin, H.; Xu, L.; Wang, L.; Kuang, H.; Xu, C. A PCR based Magnetic Assembled Sensor for Ultrasensitive DNA Detection. *Chem. Commun. (Cambridge, U. K.)* **2013**, *4*, 5369−5371.

(34) Ping Chen, Y.; Qi, C.; Xie, M. X.; Wang, D.-N.; Wang, Y. F.; Xue, Q.; Li, J. F.; Chen, Y. Immunosensor based on Magnetic Relaxation Switch and Biotin−streptavidin System for the Detection of Kanamycin in Milk. *Biosens. Bioelectron.* **2012**, *39*, 112−117.

(35) Xu, Z.; Kuang, H.; Yan, W.; Hao, C.; Xing, C.; Wu, X.; Wang, L.; Xu, C. Facile and Rapid Magnetic Relaxation Switch Immunosensor for Endocrine-disrupting Chemicals. *Biosens. Bioelectron.* **2012**, *32*, 183−187.

(36) Kodama, R. Magnetic Nanoparticles. *J. Magn. Magn. Mater.* **1999**, *200*, 359−372.

(37) Lu, A. H.; Salabas, E.e.L.; Schüth, F. Magnetic Nanoparticles: Synthesis, Protection, Functionalization, and Application. *Angew. Chem., Int. Ed.* **2007**, *46*, 1222−1244.

(38) Ito, A.; Shinkai, M.; Honda, H.; Kobayashi, T. Medical Application of Functionalized Magnetic Nanoparticles. *J. Biosci. Bioeng.* **2005**, *100*, 1−11.

(39) Lee, J. H.; Huh, Y. M.; Jun, Y. W.; Seo, J. W.; Jang, J. T.; Song, H. T.; Kim, S.; Cho, E. J.; Yoon, H. G.; Suh, J. S. Artificially Engineered Magnetic Nanoparticles for Ultra-sensitive Molecular Imaging. *Nat. Med.* **2006**, *13*, 95−99.

(40) Lu, H.; Yi, G.; Zhao, S.; Chen, D.; Guo, L. H.; Cheng, J. Synthesis and Characterization of Multi-functional Nanoparticles Possessing Magnetic, Up-conversion Fluorescence and Bio-affinity Properties. *J. Mater. Chem.* **2004**, *14*, 1336−1341.
(41) Zhao, Z.; Huang, D.; Yin, Z.; Chi, X.; Wang, X.; Gao, J. Magnetite Nanoparticles as Smart Carriers to Manipulate the Cytotoxicity of Anticancer Drugs: MagneticControl and pH-responsive Release. *J. Mater. Chem.* **2012**, *22*, 15717−15725.